International Journal of Chronic Obstructive Pulmonary Disease Dovepress
open access to scientific and medical research

Open Access Full Text Article

ORIGINAL RESEARCH

# Development of Aging-Related Emphysematous and Lymphoma-Like Lesions is Enhanced by the Lack of Secretoglobin 3A2 in Mouse Lungs

Reiko Kurotani[1], Akira Kurumazuka[1], Satoshi Sakahara[1], Kei Takakura[1], Yutaro Yokoyama[1], Lei Xu[2], Jieqiong Dai[3], Maxwell P Lee[3], Nobue Kumaki[4], Hiroyuki Abe[1], Shioko Kimura[2]

[1]Biochemical Engineering, Graduate School of Science and Engineering, Yamagata University, Yonezawa, Yamagata, 992-8510, Japan; [2]Laboratory of Metabolism, National Cancer Institute, National Institutes of Health, Bethesda, MD, 20892, USA; [3]Laboratory of Cancer Biology and Genetics, National Cancer Institute, National Institutes of Health, Bethesda, MD, 20892, USA; [4]Department of Pathology, Tokai University School of Medicine, Isehara, Kanagawa, 259-1193, Japan

Correspondence: Reiko Kurotani, Biochemical Engineering, Graduate School of Science and Engineering, Yamagata University, 4-3-16 Jonan, Yonezawa, Yamagata, 992-8510, Japan, Tel +81-238-26-3365, Fax +81-238-26-3365, Email kurotanir@yz.yamagata-u.ac.jp

**Background:** Secretoglobin (SCGB) 3A2 is a novel bioactive molecule with anti-inflammatory and anti-fibrotic activities. SCGB3A2 also promotes the maturation of bronchial divergence and the lungs during embryonic development. However, much remains unknown concerning the roles of SCGB3A2 in diseases associated with aging.

**Methods:** The lungs of *Scgb3a2*-knockout (KO) mice and their wild-type (WT) littermates were subjected to histological analysis, Victoria blue staining to evaluate of elastic fibers, and lung morphometric analysis during the postnatal period (birth to 8 weeks) and during aging (8 weeks to 2 years). Their spleens were also histologically evaluated. The expression of lung surfactant protein (SP) mRNAs was examined by quantitative reverse transcriptase-polymerase chain reaction. RNA sequencing (RNAseq) analysis was performed on 3-month-old KO and WT mouse lungs.

**Results:** The alveolar spaces of KO mice continuously expanded between 0.5 and 2 years of age, accompanied by increases of the mean linear intercept and destructive index. KO mouse lungs displayed inflammation associated with lymphocyte aggregate starting at 1 year of age, and the inflammation was worse than that of WT mouse lungs. A high number of lymphoma-like cells were presented in 2-year-old KO mouse lungs. White pulp fusion was detected in the spleens of both WT and KO mice older than 0.5 years; however, the fusion was more severe in KO mice than in WT mice. The expression of surfactant protein (SP)-A, SP-B, SP-C, and SP-D mRNAs in KO mouse lungs decreased with age, and after 1 year of age, the expression of most SPs was significantly lower in KO mice than in WT mice. RNAseq demonstrated that the expression of immune system-related genes was highly altered in KO mouse lungs.

**Conclusion:** SCGB3A2 may be required for maintaining homeostasis and immune activity in the lungs during aging. SCGB3A2 deficiency might increase the risk of emphysema of the lung.

**Keywords:** secretoglobin 3A2, aging, pulmonary emphysema

## Introduction

Secretoglobin (SCGB) 3A2, previously called uteroglobin-related protein 1 (UGRP1[1]), was identified as a downstream target of the homeodomain transcription factor NKX2-1, a key transcription factor involved in lung development and the expression of lung-specific genes.[2] SCGB3A2 is an approximately 10-kDa cytokine-like protein that exists in dimers and/or tetramers,[3] and it is primarily secreted by airway epithelial Club cells.[1] SCGB3A2 has an anti-inflammatory activity,[4] it improves pulmonary fibrosis,[5–7] and it promotes the regeneration of epithelial cells and development of embryonic lungs.[6,8] A recent study demonstrated that SCGB3A2 forms a complex with lipopolysaccharide (LPS) and chaperons LPS into the cytosol through binding with the SCGB3A2-specific cell surface receptor syndecan-1, followed by endocytosis. The internalized LPS activates the caspase-11 (4/5 in humans)-dependent non-canonical inflammasome

Received: 23 July 2021
Accepted: 30 April 2022
Published: 26 May 2022

pathway, leading to pyroptosis (inflammatory cell death).[3,9] This indicates that SCGB3A2 also functions as an immune cell-independent defense mechanism against pathogens that enter the lungs.[3]

SCGB1A1, the founding member of the SCGB family, is also known as uteroglobin, Club cell secretory protein, or Club cell 10-kDa protein (CC10), and it has been demonstrated to exert anti-inflammatory activity in the lungs and to function in immune regulation, such as the inhibition of neutrophil migration and tumor suppression.[10–12] Pathways directly involved in antigen presentation, antiviral immunity, and inflammation in alveolar macrophages were significantly suppressed in *Scgb1a1*-deficient mice compared with age-matched normal mice, suggesting that SCGB1A1 plays an important role in the formation of alveolar macrophage-mediated inflammation and immune responses.[13] Thus, SCGB family proteins may be important for the maintenance of lung homeostasis, immunity, and the development of lung, and respiratory diseases.

In C57BL/6 mice, starting immediately after birth and persisting until 2 years of age, lung compliance, lung volume, and the mean linear intercept (Lm), as indicators of lung function, increase with age, resulting in decreased airway resistance, similar to changes reported in human lungs.[14,15] In humans, the total levels of collagen and elastin in the lungs are not changed by aging, whereas it is believed that changes in the lung parenchyma are caused by changes in the connective tissue of the lungs.[16] Elastin is an evolutionarily conserved protein in vertebrates that plays a major role in mechanical properties, such as lung and vascular flexibility. Elastin is essential in lung tissue, and homozygous elastin-deficient mice die within the first few days of life.[17] The half-life of human elastin is estimated at approximately 70 years.[18–20]

It remains unclear whether SCGB3A2 plays any role in neonatal development/maturation and aging in the lungs in mice. The relationships of SCGB3A2 with elastin and other surfactant proteins (SPs) concerning the morphogenesis and structure of the lungs are also unknown. In this study, we examined the role of SCGB3A2 in the lungs during neonatal development/maturation and aging using genetically modified *Scgb3a2*-knockout (KO) mice and wild-type (WT) littermates as controls over the period from birth (day 0) to 2 years old.

# Materials and Methods

## Animals

*Scgb3a2*-KO mice on the C57BL/6N background and WT littermates (0, 1, 5, 7, and 15 days; 8 weeks; and 0.5, 1, 1.5, and 2 years old) were used in this study. Unless otherwise noted, at least four animals were used for each age group, and equal numbers of males and females were analyzed. *Scgb3a2*-KO mice were previously described.[21] Mice were housed in plastic cages in a controlled room at a temperature of 22–24°C and provided clean food and water. The lighting in the room was automatically turned on and off every 12 h. Animal experiments were conducted after approval from the Yamagata University Animal Experiment Committee. The research has been carried out in accordance with the Guidelines for Proper Conduct of Animal Experiments (Science Council of Japan) and international guiding principles for biomedical research involving animals.

## Lung Sample Preparation

All mice were anesthetized by an intraperitoneal administration of somnopentyl (64.8 mg/kg) (Kyoritsu Pharmaceutical, Tokyo, Japan). Blood was collected from the inferior vena cava and centrifuged at 5000 rpm at 4°C for 5 min to prepare serum. Lung tissue was gently lavaged three times with 0.5 mL of phosphate-buffered saline (PBS) through a tracheal cannula, and bronchoalveolar lavage fluid was obtained. The left main bronchus was then ligated, and the left lung was excised and halved. One half of the lung was immersed in TRIzol (Thermo Fisher Scientific, Waltham, MA, USA) for RNA extraction, and the other half was placed in lysis buffer [25 mM Tris-base, 10 mM EGTA, 10 mM EDTA 0.1% NP-40, and 1× protease Inhibitor cocktail (Thermo Fisher Scientific)] for protein extraction. The remaining right lung tissue was fixed intratracheally with 4% paraformaldehyde (PFA) in 0.1% phosphate buffer (PB), pH 7.4 under a constant pressure of 25 $cmH_2O$ for histological analysis. For mice aged 0, 1, 5, 7, and 15 days, all lung lobes were resected and processed for histological analysis or gene expression analysis. Spleen was extracted, photographed, and fixed in 4% PFA in PB. All tissues were fixed for 16–24 h.

## Morphology

The paraffin-embedded sections of mouse lungs and spleens were sliced at a thickness of 4 μm for histological examination. For lungs, hematoxylin and eosin (HE) staining was performed to evaluate tissue histopathology and determine the mean linear intercept (Lm) and the destructive index (DI), whereas Victoria blue (VB) staining was performed to detect elastin. The evaluation method for elastin was described in the Supplemental Materials and Methods. Five transverse lines were drawn per visual field (×200 magnification), and Lm was calculated by dividing the length (L) of the transverse line by the number of times (m) the transverse line was interrupted by the alveolar wall [Lm = 5 × L/m (μm)].[22–24] To determine DI, 50 points arranged at equal intervals were overlaid onto issue images. Alveoli located below the points were regarded as destroyed if they met at least one of the following criteria: (1) at least two defects in the alveolar wall, (2) two or more parenchymal fragments in the alveolar lumen, (3) obvious morphological abnormalities, and (4) classic emphysematous changes. DI was calculated by dividing the number of destroyed alveoli by the total number of alveoli.[23,24] Lm and DI were evaluated for 10 visual fields per mouse.

Immunohistochemistry (IHC) was performed to evaluate expression of SCGB3A2 and Ym1/2, a marker of macrophage pneumonia[25] and type II macrophages,[26] in the lungs. In brief, after deparaffinization, sections were washed with pure water and immersed in 0.3% $H_2O_2$ in methanol for 30 min at room temperature to inactivate endogenous peroxidase in the tissue. Tissue was then heated in a citrate buffer (pH.6.0) for 10 min at 750 W power, using a microwave oven for antigen activation. Citrate buffer was cooled, and the sections were reacted with 5% milk (Morinaga Milk, Tokyo, Japan) in PBS (pH 7.4) for 1 h at room temperature to block nonspecific proteins. Primary antibodies against mUGRP1 (same as SCGB3A2, AF3465, R&D Systems, Minneapolis, MN, USA) or Ym1/2 (ab192029, Abcam, Cambridge, MA, USA) diluted 2000-fold with 5% milk in PBS were reacted with the slides at 4°C for 16–18 h. After the primary antibody reaction, biotin-labeled secondary antibody, supplemented with normal (rabbit or goat) serum was added to the tissues and reacted for 30 min at room temperature followed by reaction with HRP-labeled avidin and biotin complex for 30 min at room temperature in the dark (Vectastain Elite ABC Kit, Vector Laboratories, Burlingame, CA, USA). SCGB3A2 and Ym1/2 were visualized using 3, 3′-diaminobenzidine (DAB) (Dako Japan, Tokyo, Japan), counterstained with hematoxylin for 1 min to visualize the nucleus, and then immersed in warm water at 60°C. The stained tissue specimens were observed using an upright BX51 microscope (Olympus, Tokyo, Japan), and the tissue images were captured using a DP51 digital camera (Olympus). The expression and localization of SCGB3A2 and Ym1/2 in the lung tissues were then assessed. All histological observations were made by two to three investigators from different laboratories blinded to genotype, age in weeks, and sex.

## Quantitative Reverse Transcriptase-Polymerase Chain Reaction (qRT-PCR)

The left lung of each mouse was crushed in 2 mL of TRIzol using a homogenizer (Hiscotron, NS-52, Microtechnion, Chiba, Japan) to form a suspension, and total RNA was extracted according to the manufacturer's protocol. The total RNA concentration and purity were measured using a spectrophotometer (NanoDrop-1000, Thermo Fisher Scientific). The removal of genomic DNA from total RNA and the reverse transcription reaction were performed using a PrimeScript reagent kit with gDNA Eraser (Takara Bio, Shiga, Japan) according to the manufacturer's instruction. The expression of representative lung-specific genes was analyzed by qRT-PCR using an Mx-3000P system (Agilent Technologies, CA, USA) and SYBR® Premix Ex Taq™ II (Takara) with the primers presented in Supplemental Table S1. The conditions used were as follows: 95°C for 30s; 40 cycles of 95°C for 10s and 60°C for 30s; and as an additional cycle of 95 °C for 60s, 55 °C for 30s, and 95 °C for 30s. The standard curve method was used, and all data were normalized to β-actin expression.

## RNA Sequencing (RNAseq)

RNAs purified from the lungs of *Scgb3a2*-null and corresponding WT mice (3-month-old males) were subjected to RNAseq on a HiSeq2500 system using an Illumina TruSeq v4 chemistry kit (https://www.illumina.com/) by the NCI sequencing core (Frederick, MD, USA). Sequencing reads were mapped to mouse genome mm10. The HTseq[27] module was used for counts calling from the bam files. Data processing was performed using the computational resources of the

NIH HPC Biowulf cluster (http://hpc.nih.gov). Sequencing read counts were input to RStudio (https://rstudio.com/) and further analyzed using the Deseq2 package[28] (https://github.com/mikelove/DESeq2). Data normalization, annotation, and differential expression analysis were conducted using the Deseq2 package. The heatmap plot was created using the gplots package (https://github.com/cran/gplots). Genes in KO samples with 2-fold changes in expression versus the control level and p value less than 0.01 were selected for downstream analysis. Signaling pathways were enriched using the online software Metascape (https://metascape.org).[28] The RNAseq data have been submitted to the NCBI Gene-Expression Omnibus under GEO accession number GSE186515.

## Statistical Analysis

The values obtained from the experiments are presented as the mean ± standard deviation (SD). Significant differences were assessed by performing one-way analysis of variance (ANOVA), followed by the Tukey–Kramer post hoc test among multiple groups and Student's *t*-test between two groups. Differences were considered significant at $p < 0.05$.

Information on additional methods, Evaluation of elastic fiber content, Cell culture, and Fluorescent immunostaining, are provided in the Supplemental Materials and Methods in the Supplemental information.

# Results

## Lung Morphology During Neonatal Development/Maturation

To examine the effect of SCGB3A2 on lung development/maturation, lung tissues from WT and *Scgb3a2*-KO mice were examined at various ages from 0 to 15 days and 8 weeks. The lungs of WT and KO mice on day 0 displayed underdeveloped structures, with thick alveolar walls and large alveolar cavities (Figure 1A i and ii). As pulmonary structures in mice require approximately 30 postnatal days to mature,[29] the alveolar wall gradually became thinner and the alveolar cavity became smaller during the first 15 postnatal days (Figure 1A i–x). At day 15, alveolar formation in WT and KO mice was similar to that observed in 8-week-old mature lungs (Figure 1A i–xii), whereas the alveolar spaces of the 8-week-old KO mouse lungs appeared to be slightly enlarged compared to those of their WT counterpart (Figure 1A xi and xii). VB staining, which detects connective tissue, elastic fibers, and fibrosis, was then performed to determine the elasticity of lung tissue (Figure 1B). Positive VB staining was observed in the basement membrane of blood vessels, trachea, and alveoli in both WT and *Scgb3a2*-KO mouse lungs. The intensity of VB staining in the alveolar epithelia increased from 0 to 15 days, and the staining patterns were similar between 15 days and 8 weeks and between the two genotypes (Figure 1B i–xii). Image analysis of alveolar elastin levels from 0 day to 2 years showed that alveolar elastin clearly began to increase on day 15 and remained at similar levels from 8 weeks through 2 years of age (Supplemental Figure S1). Apparent differences were found in the elastin signal intensity between alveolar epithelia from WT and KO mice at most ages, with KO alveolar epithelia in general having slightly stronger intensity. Conversely, the blue signals in the vascular basement membrane and the trachea of both WT and KO mouse lungs were comparable at most ages (Figure 1B). Immunohistochemical analysis confirmed the expression of SCGB3A2 in the bronchial epithelial cells of WT mice from day 0 to 8 weeks and 1 year (Supplemental Figure S2Ai–vii). No SCGB3A2 expression was observed as expected in KO mouse lungs (Supplemental Figure S2Aviii). In addition, qRT-PCR illustrated that *Scgb3a2* mRNA expression was low from day 0 to day 7, with apparent increases at day 15 and further increases at 8 weeks (Supplemental Figure S2B). These results demonstrated that SCGB3A2 deficiency does not affect the maturation of postnatal lung morphogenesis.

## Lung Morphology During Aging Process

To clarify the effects of SCGB3A2 on lung morphology and function during aging, lung tissues obtained from WT and *Scgb3a2*-KO mice at the ages of 8 weeks and 0.5, 1, 1.5, and 2 years were examined. *Scgb3a2*-KO mice (71%) had a similar 2-year survival rate as WT mice (69%). In WT mice, the alveolar space in lung tissue did not increase remarkably from 8 weeks to 1 year of age (Figure 2A i, iii, and v), whereas in *Scgb3a2*-KO mice, the alveolar space appeared to be slightly enlarged at 8 weeks of age (Figure 2A ii), with continued enlargement from 0.5 to 2 years of age compared with that in WT mice (Figure 2A iii–x). VB staining was performed to determine the elasticity of aging lung tissues of WT and

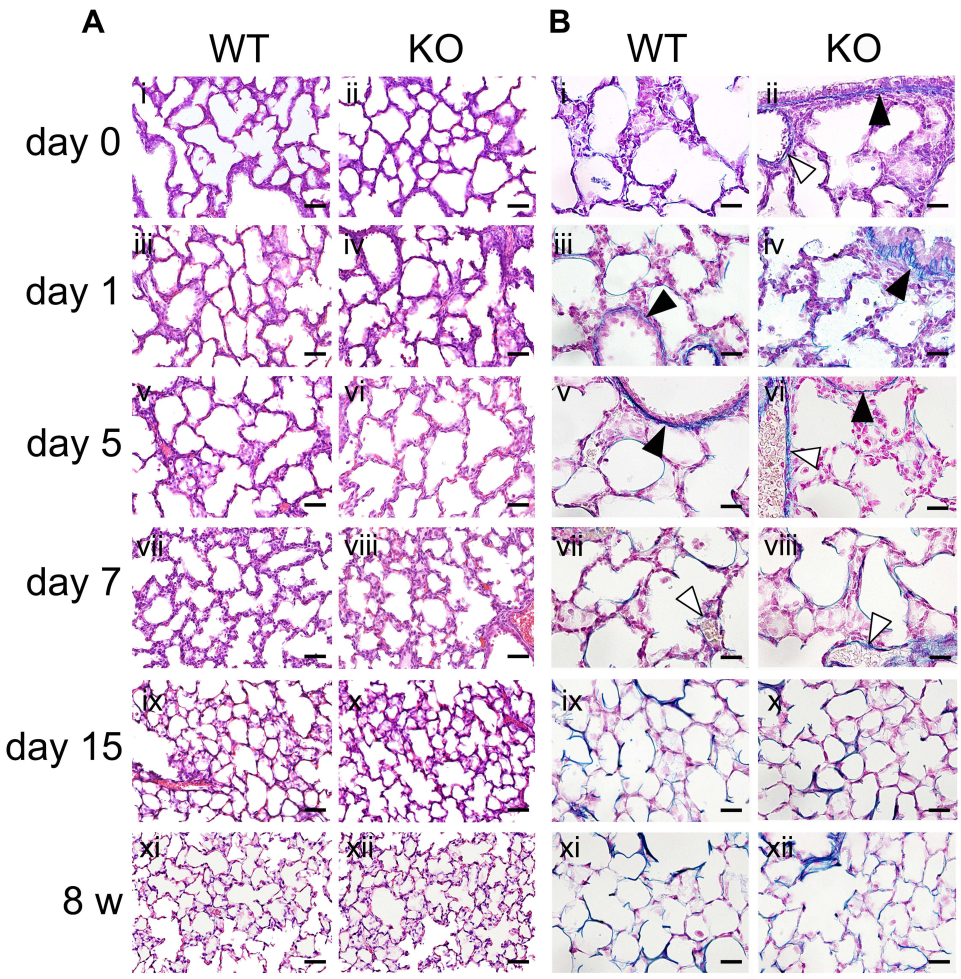


**Figure 1** Morphology and elastic fiber formation in the lungs during development/maturation. (**A**) Representative hematoxylin and eosin (HE)-stained staining images of lung tissues from wild-type (WT) and *Secretoglobin* (*Scgb*) *3a2*-knockout (KO) mice from birth (day 0) to 8 weeks of age (8 w) (i–xii). Neonatal alveolus formation and alveolar development were observed from day 0 to day 15 (i–x), in line with the histology observed in 8-week-old mouse lungs (xi and xii). Scale bars: 50 μm. (**B**) Representative Victoria blue (VB) staining of lung tissues from WT and *Scgb3a2*-KO mice from birth (day 0) to 8 weeks of age (8 w) (i–xii). Alveolar elastin staining increased from day 0 to day 15 (i–x), and the intensity remained similar between day 15 (ix and x) and 8 w (xi and xii). Blue: VB elastin staining; black arrowheads: basement membranes of bronchi; white arrowheads: basement membranes of blood vessels. Scale bars: 20 μm.

*Scgb3a2*-KO mice (Figure 2B). As mice aged from 1 to 2 years, the intensity of VB staining in the basement membrane of pulmonary alveoli of WT mouse lungs gradually decreased (Figure 2B i, iii, and v), whereas decreased VB staining and the destruction of alveolar elastin fiber were evident in *Scgb3a2*-KO mouse lungs (Figure 2B ii, iv, and vi).

To quantify whether SCGB3A2 deficiency affected alveolar cavity expansion in addition to the tissue changes presented in Figure 2A and B, Lm and DI were measured as indicators of lung morphological changes in WT and *Scgb3a2*-KO mouse lungs (Figure 3). Lm in WT mice remained constant from 8 weeks to 1.5 years old and increased significantly at 2 years old (Figure 3A). Conversely, *Scgb3a2*-KO mice exhibited similar Lm from 8 weeks to 0.5 years, and the value then became significantly larger than that in WT mice after 1 year (Figure 3A). In addition, DI was significantly larger in *Scgb3a2*-KO mice than in WT mice at any age from 8 weeks to 2 years old, and the values further increased after an age of 1 year (Figure 3B). DI remained constant in WT mouse lungs throughout the aging process. These results demonstrated that *Scgb3a2* deficiency contributed to the destruction of lung alveolar structures during aging.

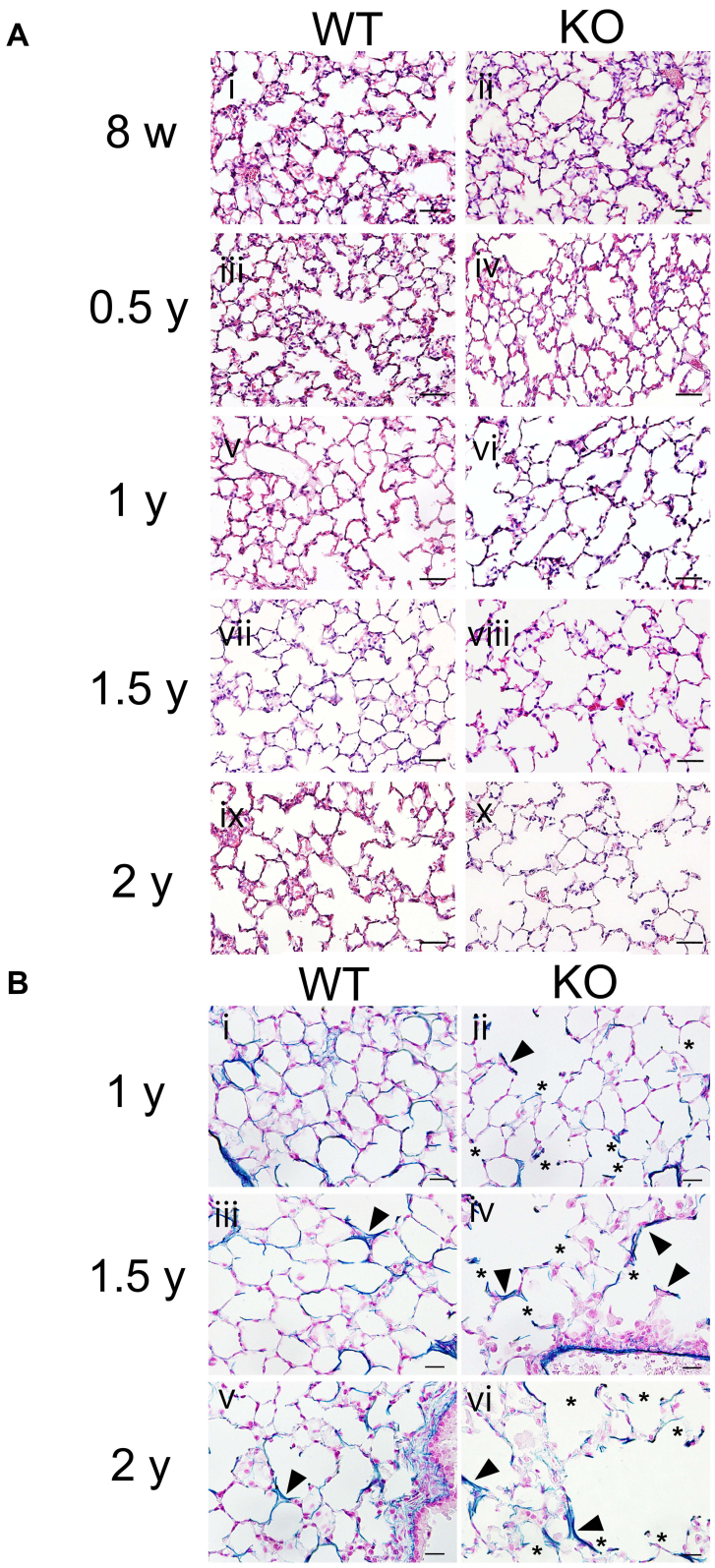


**Figure 2** Morphology and elastic fiber formation in the lungs during aging process. (**A**) Representative hematoxylin and eosin (HE)-stained images of lung tissues from wild-type (WT) and *Secretoglobin* (*Scgb*) *3a2*-knockout (KO) mice at 8 weeks old (8 w) and from 0.5 to 2 years old (0.5–2 y) (i–x). In WT mouse lungs, the expansion of the alveolar cavity was occasionally observed in the lungs of 1.5 y and 2 y. Conversely, in *Scgb3a2*-KO mouse lungs, more numbers of alveoli with remarkable cavity expansion were observed after 1 year of age (1 y) (vi, viii, and x). Scale bars: 50 μm. (**B**) Representative Victoria blue (VB) staining of lung tissues from WT and *Scgb3a2*-KO mice from 1 year (1 y) to 2 years (2 y) of age (i–vi). In both WT and KO lungs, some of cleaved alveolar walls were stained dark blue stain by VB staining (arrowheads). A high degree of elastin fiber destruction was observed in the alveoli of KO mouse lungs (ii, iv, and vi). Asterisk (*): elastin fiber destruction, Blue: VB elastin staining, Scale bars: 20 μm.

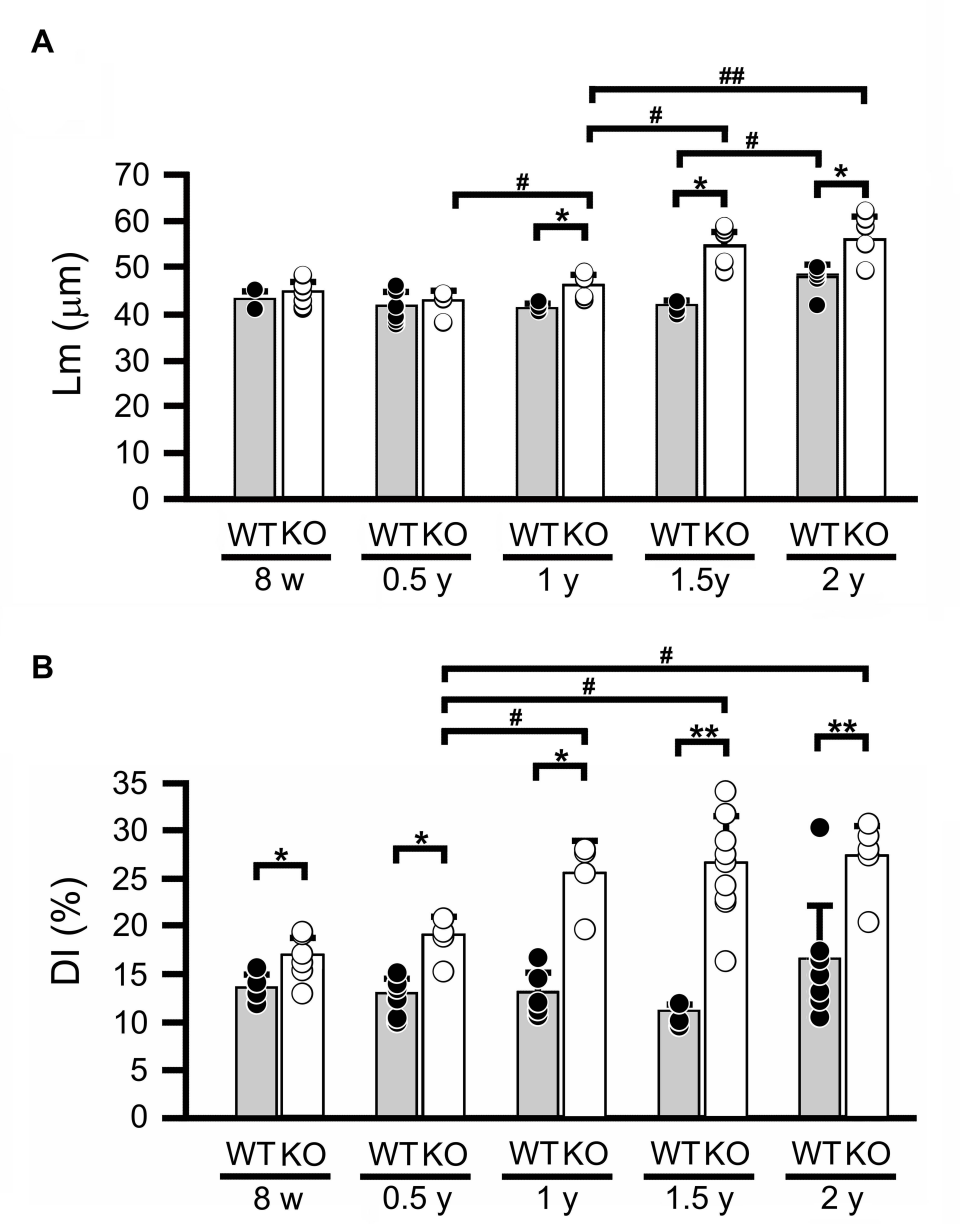


**Figure 3** Lm and DI in lung tissues during aging. (**A**) Mean linear intercept (Lm) in wild-type (WT) and *Secretoglobin* (*Scgb*) *3a2*-knockout (KO) mouse lungs from 8 weeks (8 w) to 2 years of age (2 y). Lm of WT significantly increased in 2-year-old (2 y) in WT mice, whereas that in KO mice gradually increased after 1 year (1 y), being significantly larger than that in WT. (**B**) Destructive index (DI) in wild-type and *Scgb3a2*-KO mouse lungs from 8 w to 2 y. DI was constant regardless of age in WT mice, and after 1 year of age (1 y) in KO mice. Filled columns and black dots: WT; open columns and white dots: KO; N=5-9. Specifically, the number of mice analyzed were as follows: WT [8w: 3 males (m), 2 females (f); 0.5y: 4m, 4f; 1y: 3m, 2f; 1.5y: 5f; 2y: 3m, 5f] and KO (8w: 4m, 3f; 0.5y: 3m, 4f; 1y: 2m, 2f; 1.5y: 5m, 4f; 2y: 3m, 3f). Because Lm and DI did not apparently differ between male and female mice, the results were combined. Data are presented as the mean ± standard deviation (SD). Statistical differences between ages in the same strain were analyzed by one-way analysis of variance (ANOVA), followed by the Tukey–Kramer post hoc test ($^{\#}p < 0.05$, $^{\#\#}p < 0.01$). Differences between different strains at the same age were analyzed using Student's *t*-test ($^{*}p < 0.05$, $^{**}p < 0.01$).

## Pathological Changes in *Scgb3a2*-KO Lungs with Aging

*Scgb3a2*-KO mouse lungs were examined for pathological changes associated with aging other than alveolar structure destruction. Mild lymphocyte aggregation was observed in more than half of WT mice after 1 year of age (Figure 4A i 2-year-old of WT lung, Supplemental Table S2), whereas in KO mice, several marked lymphocyte aggregation was observed in most lungs after 1.5 years of age (Figure 4A ii–iv; 2-year-old of KO lung, Supplemental Table S2). In addition, atypical lymphocytes and/or lymphoma-like cells were observed in some older KO mouse lungs (Figure 4A iv).

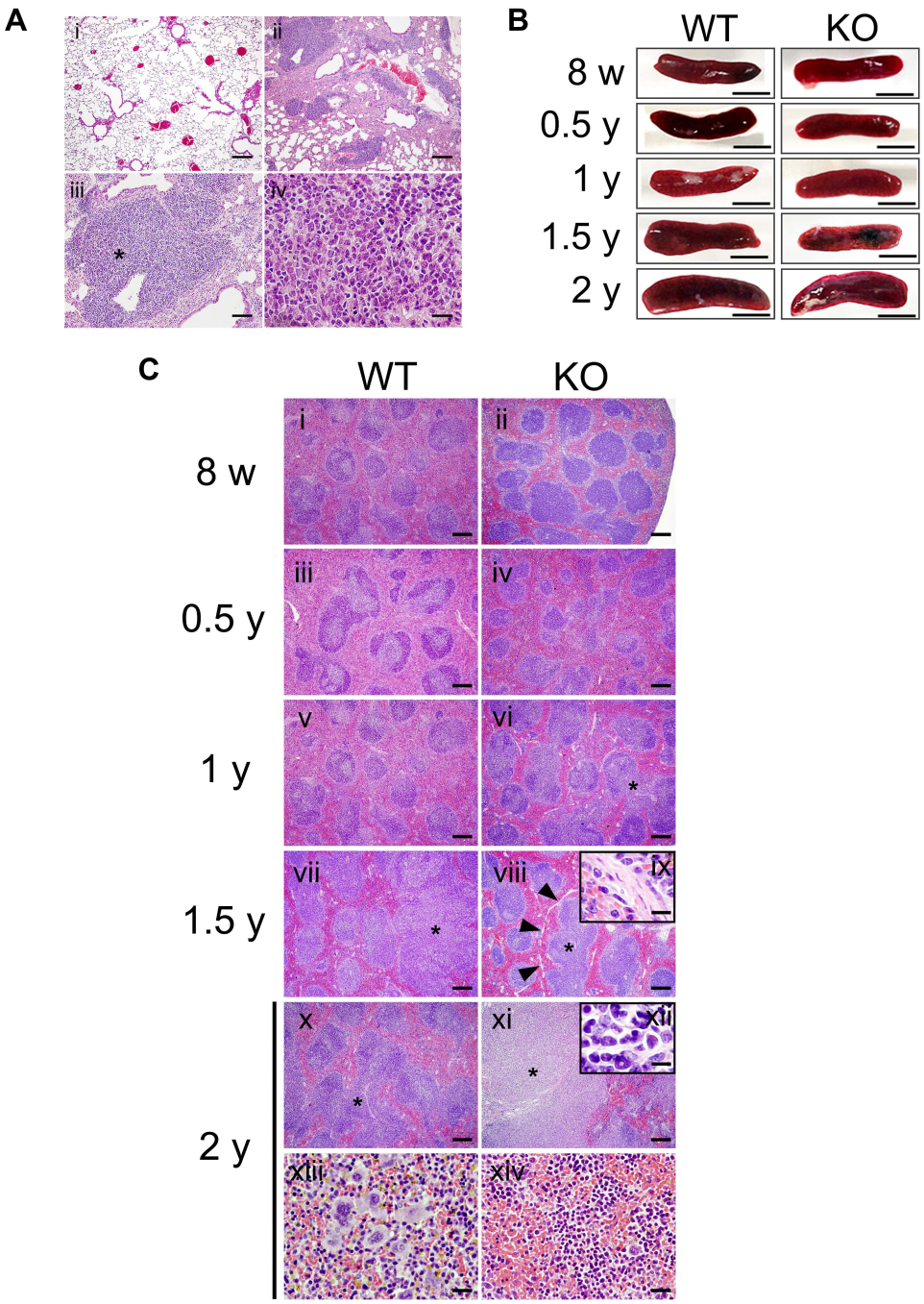


**Figure 4** Pathological changes in the lungs and spleens of mice with aging. (**A**) Representative hematoxylin and eosin (HE)-stained images of aged wild-type (WT) and *Secretoglobin* (*Scgb*) *3a2*-knockout (KO) mouse lungs. (i) Two-year-old WT mouse lungs exhibiting mild lymphocyte aggregation. (ii) Marked lymphocyte aggregation detected in 2-year-old KO mouse lungs. (iii) Atypical lymphocytes observed in 2-y-old KO mouse lung. Scale bars: 200 μm. (iv) Enlarged photo near the asterisk in c. Scale bar: 20 μm. (**B**) Macroscopic observations and diameters of spleens measured in senescent WT and *Scgb3a2*-KO mice. Representative spleens are presented. Scale bars: 5 mm. (**C**) Representative histological observations of spleen tissues from WT (i, iii, v, vii, x, and xiii) and *Scgb3a2*-KO mice (ii, iv, vi, viii, xi, and xiv) at various ages. In the spleen of 2-year-old KO mice, remarkable fusion of white pulp (xi) and a highly malignant image (ix: inset, ×1000) were observed. Asterisk (*): white pulp fusion; arrowheads: fiber formation; ix: enlargement of arrowheads in viii; xii: enlargement of * in xi; xiii: extramedullary hematopoiesis (erythroid element, megakaryocytes, and myeloid cells) in the splenic red pulp; xiv: erythropoiesis in red pulp. Scale bars: 200 μm (i–viii, x, and xi), 50 μm (xiii, xiv), and 10 μm (ix, xii).

Alveolar hyperplasia, lymphoma, and lymphoma-like lesion were also observed in KO mouse lungs after 1 year of age (Supplemental Table S2).

Although C57BL/6 mice are known to be prone to develop lymphoma with aging,[30] the degree of inflammation in the lungs tended to be more severe in KO mice (Figure 4A ii–iv, Supplemental Table S2). There were cases of macrophage

pneumonia in a 1.5-year-old WT mouse (Supplemental Figure S3Ai and iii) and a 2-year-old KO mouse (Supplemental Figure S3Aii and iv). Considering the number of cases, it is unlikely that macrophage pneumonia was caused by SCGB3A2 deficiency. However, because Ym1 is a marker for type II macrophages,[26] the effect of SCGB3A2 on macrophage polarity was examined by determining macrophage marker gene expression in macrophage cell lines with and without SCGB3A2 by qRT-PCR (Supplementary Figure S3Bi–iv). The mRNA expression of TNF-α (marker for type I macrophages) and IL-10 (marker for type II macrophages) was significantly decreased and increased, respectively, in Raw264 mouse macrophages and MH-S alveolar macrophages in the presence of SCGB3A2. Although the relationship between the presence of SCGB3A2 and macrophages in the lungs of aging mice is unknown, it was suggested that SCGB3A2 changes the polarity of macrophages from type I to type II.

## Tissue Histopathology of the SCGB3A2-Deficient Mouse Spleen During Aging

It was possible that the high level of lymphocyte aggregation observed in the lungs of *Scgb3a2*-KO mice may represent lymphoma. Therefore, the spleen, the site of lymphocyte maturation, was examined. Splenic gross observation and the long diameter measurement were carried out from 8 weeks through 2 years of age in WT and *Scgb3a2*-KO mice (Figure 4B and Table 1). The spleen sizes increased with aging, but no differences were detected between WT and KO mice at any ages, except 1.5 years old where the KO spleen size was statistically significantly smaller than WT mice (Figure 4B and Table 1). In the WT mouse spleens, few morphological abnormalities were observed from 8 weeks to 1 year of age (Figure 4C i iii, and v), while white pulp fusion became clearly visible at 1.5 and 2 years old (Figure 4C vii and x, Supplementary Table S3). In particular, areas of prominent extramedullary hematopoiesis in splenic red pulp was observed in the spleens of 2-year-old WT mice (Figure 4C xiii, Supplemental Table S3) as well as KO mice (data not shown). Similarly, few morphological abnormalities were observed in the spleens of KO mice from 8 weeks to 0.5 years of age (Figure 4C ii and iv), and the white pulp fusion was found at 1 year of age (Figure 4C vi). The fusion became remarkable at 1.5 and 2 years of age (Figure 4C viii and xi), which coincided with the lymphocyte aggregation in the lungs (Figure 4A ii and iii, Supplemental Table S2). In the spleens of KO mice, fibrosis around the white pulp became noticeable at 1.5 years of age (Figure 4C viii and ix), and erythropoiesis was also observed, becoming remarkable at 2 years of age (Figure 4C xiv). At 2 years of age, the presence of atypical lymphocytes in the white pulp was confirmed (Figure 4C xii).

## Expression of Lung-Specific Genes During Aging Process

To understand the possible underlying mechanism for the development of destructive alveoli and inflammation in the lungs of *Scgb3a2*-KO mice during aging, the mRNA levels of *Scgb1a1*, SP-A (*Sftpa*), SP-B (*Sftpb*), SP-C (*Sftpc*), and SP-D (*Sftpd*) were examined by qRT-PCR (Figure 5A i–vi). *Scgb3a2* mRNA expression in the lungs of WT mice did not change during aging. Similarly, the mRNA expression of *Scgb1a1* and *Sftps* in WT lungs remained at similar levels during aging. In KO mouse lungs, *Scgb1a1* and *Sftpa* mRNA levels were unchanged during aging. However, *Sftpb* and *Sftpd* mRNA levels were significantly decreased between 1 and 1.5 years of age compared with those at 8 weeks, and *Sftpc* mRNA levels significantly decreased between 0.5 and 1 year of age. The levels of these mRNAs in KO lungs were generally lower than those in WT lungs, particularly when they age. *Scgb1a1* mRNA levels were significantly lower in KO mice than in WT mice at 2 years of age. *Sftpa* mRNA levels were significantly lower in KO lungs at 8 weeks, 1 year, and 1.5 years of age, whereas those of *Sftpb* were significantly lower from 0.5 through 2 years of age. *Sftpc* and *Sctpd* mRNA levels were both significantly lower in KO lungs than WT at 1 and 1.5 years of age. In addition, the protein expression of SPs in bronchial epithelial cells at each age was examined by fluorescence immunostaining. The results demonstrated that the fluorescence signal of each SP in the lungs of KO mice clearly decreased with age (Supplemental Figure S4Ai–x–Di–x), similar to the results of qRT-PCR. The expression of the alpha-1-antitrypsin (A1AT) gene, *Serpina1a*, the deficiency of which is known to cause pulmonary emphysema,[31,32] was also examined by qRT-PCR. The results illustrated that *Serpina1a* mRNA was detected in 8-week-old WT mouse lungs, but almost undetectable in 8-week-old KO mouse lungs, suggesting that SCGB3A2 may affect *Serpina1a* expression (Supplemental Figure S5). To further investigate the fundamental gene expression differences between WT and KO mice, RNAseq of lungs from 3-month-old mice was performed (Figure 5B). At this age, there were no differences in the expression of the

**Table 1** Longer Axis (mm) in the Spleen of the WT and *Scgb3a2*-KO Mice

| Age / Genotype | 8 w | 0.5 y | 1 y | 1.5 y | 2 y |
|---|---|---|---|---|---|
| WT | 13.35±0.71 (4) | 13.86±0.79 (3) | 14.27±0.37 (9) | 15.47±0.27 (5)# | 16.77±0.75 (6)# |
| KO | 13.66±0.23 (8) | 13.41±0.33 (4) | 14.06±0.62 (4)# | 13.64±0.68 (3)* | 16.57±1.34 (4)# |

**Notes**: Numbers in parenthesis show the number of samples. Tukey-Kramer post hoc test and Student's *t*-test were respectively carried out to determine a significance among different ages of same genotype mice (WT or KO), and between the two groups (WT vs KO) of same age. The significant difference were # $p<0.05$ for 1.5 and 2 yrs of WT, or 1 or 2 yrs of KO vs each corresponding remaining age groups * $p<0.05$ between WT vs KO at 1.5 y of age. WT: wild-type, KO: *Secretoglobin* (*Scgb*) *3a2*-knockout, 8 w: 8 weeks old, 0.5 y to 2y: 0.5 years old to 2 years old.

aforementioned genes excluding *Scgb3a2* between WT and KO lungs (Supplemental Figure S6). Gene Ontology (GO) analysis revealed significant changes in adaptive immune response (GO: 0002250) and immunoglobulin production (GO: 0002377), followed by antimicrobial humoral response (GO: 0019730), mononuclear cell differentiation (GO: 1903131), regulation of immune effector processes (GO: 0002697), and primary immunodeficiency (ko05340) in the lungs of KO mice compared with the findings in WT mice (Figure 5B). The heatmap demonstrated that the altered expression of genes was mainly related to the immune system in KO mouse lungs as compared with WT mouse lungs (Supplemental Figure S6). These results revealed that KO mouse lungs possess an inherently altered immune system.

## Discussion

SCGB3A2 is a low-molecular-weight bioactive cytokine-like molecule that could be considered as an SP. SCGB3A2 promotes lung bronchial branching during embryogenesis,[8] exerts anti-inflammatory effects,[4] and improves pulmonary fibrosis,[5,7] thus playing an important role in the development, function, and homeostasis of the lungs. However, much remains unknown concerning whether SCGB3A2 participates in postnatal lung maturation and the development of aging-associated diseases. This study aimed to clarify the roles of SCGB3A2 in these processes.

Early-stage neonatal alveolar development is attributed to alveolar dilation and fragmentation.[33] The histological analysis of WT and *Scgb3a2*-KO mouse lungs revealed a similar alveolar subdivision in both WT and KO mouse lungs during maturation from day 0 to 8 weeks. Because exogenous SCGB3A2 promoted bronchial branching and lung maturation,[8] we expected that *Scgb3a2* deficiency would result in abnormal lung development. However, Sc*gb3a2*-KO mice were healthy and fertile for at least 1 year, as previously reported,[21] and in this study, a majority of them survived for approximately 2 years, similarly to WT mice. No significant changes in lung histogenesis were observed in *Scgb3a2*-KO mice, although a small but statistically significant decrease in ciliated cell counts in the large airways of KO lungs has been reported.[34] The reason why *Scgb3a2*-KO mouse lungs were normal is unclear. Embryonic lung development may be slightly delayed in the absence of SCGB3A2, but these changes had normalized by day 0, the earliest time of analysis in *Scgb3a2*-KO mice. Further, because SCGB3A2 is one of many NKX2-1 downstream targets involved in lung development and homeostasis, other gene products may compensate for the lack of SCGB3A2-mediated growth promotion.[21]

Elastin staining illustrated that elastin expression increased in the lungs of both WT and *Scgb3a2*-KO mice from day 0 to 8 weeks of age. This increase was associated with the development of alveoli. Based on image analysis, the elastin signal was slightly stronger in KO mouse lungs than in WT mouse lungs at most of ages. This could simply reflect technical problems associated with tissue staining and quantification. Destroyed alveoli with damaged elastin fibers tend to stain stronger at the edge, which occurred more frequently in KO mouse lungs than in WT mouse lungs. Alternatively, SCGB3A2 might be involved in the regulation of elastin expression by a currently unknown mechanism. When Lm and DI were measured, no significant changes were observed in the alveolar structures of WT mice from the ages of 8 weeks to 2 years, except that Lm was significantly increased in 2-year-old mouse lungs, indicating aging of the lungs.[35] Contrarily, *Scgb3a2*-KO mice displayed alveolar space dilation and alveolar wall destruction, which are signs of pulmonary emphysema, after 1 year of age, and these changes significantly worsened at 1.5 and 2 years old. These results suggest that the absence of SCGB3A2 promotes emphysematous lung development.

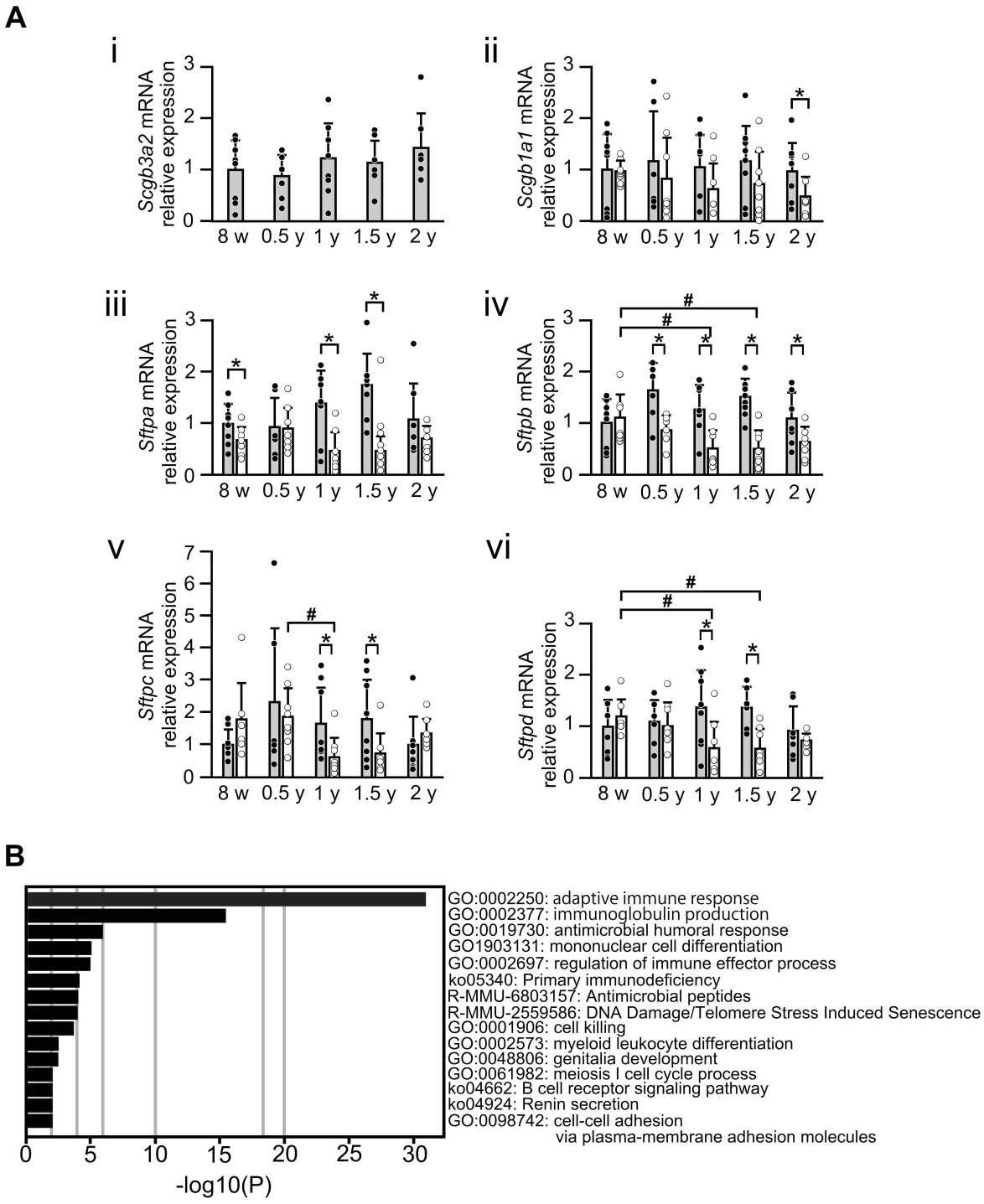


**Figure 5** Gene expression in lung tissues from WT and *Scgb3a2*-KO mice during aging. (**A**) Surfactant protein (SP) gene expression in lung tissues from wild-type (WT) and *Secretoglobin (Scgb) 3a2*-knockout (KO) mice during aging. mRNA levels coding for Secretoglobin (SCGB) 3A2, SCGB1A1, SP-A, SP-B, SP-C, and SP-D [*Scgb3a2* (i), *Scgb1a1* (ii), *Sftpa* (iii), *Sftpb* (iv), *Sftpc* (v), and *Sftpd* (vi), respectively] in the lungs of WT and *Scgb3a2*-KO mice were examined by quantitative reverse transcriptase-polymerase chain reaction (qRT-PCR) from 8 weeks (8 w) to 2 years of age (2 y). The expression of each mRNA was compared with that at 8 w in WT mice, which was set as 1. Filled column: WT; open column: KO; N = 4–8. Specifically, the number of mice analyzed were as follows: WT [8 w: 4 males (m), 4 females (f); 0.5y: 2m, 4f; 1y: 3m, 5f; 1.5y: 8f; 2y: 4m, 3f] and KO (8w: 3m, 4f; 0.5y: 3m, 5f; 1y: 3m, 5f; 1.5y: 8m; 2y: 2m, 5f). Because the mRNA expression levels did not apparently differ between male and female mice, the results were combined. Data are presented as the mean ± standard deviation (SD). Statistical differences between ages in the same strain were analyzed by one-way analysis of variance (ANOVA), followed by the Tukey–Kramer post hoc test ($^{\#}p < 0.05$). Differences between different strains at the same age were analyzed using Student's *t*-test ($^{*}p < 0.05$). (**B**) RNA sequencing (RNAseq) of 3-month-old WT and KO lungs. Gene ontology (GO) analysis was performed after RNAseq of these lungs to investigate differences in the gene expression pattern between WT and KO mouse lungs. Compared with WT mice, the expression of genes mainly related to the immune system was increased in the lungs of KO mice.

The pathological analysis of aging mouse lung tissues revealed the aggregation of lymphocytes both in WT and KO mice starting at the age of 1 year of age. Specifically, a small number of lymphocytes were noted in some WT mouse lungs, whereas a significant number of aggregated lymphocytes were found in most KO mouse lungs. C57BL/6 mice tend to develop lymphoma as they age.[30] The observation of splenic tissues revealed abnormal findings, such as the greater frequencies of the fusion of white pulp and some highly malignant lymphocytes, which were found more in KO mice than in WT mice, consistent with the previous report on aged C57BL/6 mice.[36] Related to this, it is important to note that SCGB3A2 is not normally expressed in the spleen.[1] Lymphocytes and macrophages mature in the spleen and migrate throughout the body, including the lungs.[37] Therefore, it seems that numerous lymphocyte aggregation sites in the lungs of aging KO mice may have been caused by splenic abnormalities. In fact, the white pulp fusion and highly malignant lymphocytes were observed in the spleens of KO mice with severe inflammation in the lungs. SCGB1A1 was reported to counteract neutrophil chemotaxis in airway epithelium;[12] however, there are no reports on the effect of SCGB1A1 or any other SCGB proteins including SCGB3A2 on macrophage migration. Assuming that SCGB3A2 inhibits macrophage migration similarly as SCGB1A1 inhibits neutrophil migration, macrophages mobilized in KO lungs might be affected by the spleen. Previous studies demonstrated that SCGB3A2 may affect immune cells, including macrophages.[5] Syndecan-1, a SCGB3A2 receptor, is present on the surface of macrophages, and pyroptosis is induced by SCGB3A2 in macrophages.[3] Furthermore, SCGB3A2 shifts the polarity of the macrophage toward type II, and SCGB3A2 can be detected in blood as well as bronchoalveolar lavage fluid (BALF) (Supplemental Figure S7A and B). These results suggest that SCGB3A2 secreted into blood and the lung space can enhance the immune response by interacting with macrophages present in the blood as well as tissue-specific macrophages. Macrophages may aggregate in the chronically inflamed aging emphysematous lungs of KO mice, as observed in macrophage pneumonia. In addition, increased splenic monopoiesis has been reported to respond to signals from the microenvironment.[36] Therefore, abnormally aggregated macrophages might send a signal to the spleen that interferes with its normal function.

The results of qRT-PCR demonstrated that the loss of SCGB3A2 generally resulted in the decreased expression of SP genes (*Sftpa, Sftpb, Sftpc*, and *Sftpd*) in aged lungs. SPs are known to participate in the homeostatic maintenance and immunity of lungs. It was reported that SP-D–deficient mice develop progressive emphysema with the age-related loss of parenchymal tissue, subpleural fibrosis, and aggregation of abnormal elastin fibers.[38] SP-B–deficient mice develop respiratory failure at birth, which has been revealed to be associated with decreased lung compliance.[39] Further, SPs interact with each other to regulate the expression of other SPs. For example, SP-B post-translationally modifies SP-C expression levels.[40] SP-A is known to regulate the transcription of other *Sftp* genes including *Sftpb* and *Sftpc*.[41] SP-A and SP-B directly interact,[42] and they are believed to participate in homeostasis during aging and in the immune function in the lungs.[43] Further, SP-C regulates the stability of pulmonary surfactant in the lungs,[44] and reduces inflammation.[45,46] These findings suggest that SCGB3A2 deficiency accompanied by age-related decreases of SP levels increases the risk of emphysema in aging mice. The RNAseq results support the notion that KO mouse lungs have more severe inflammation than WT mouse lungs because of the altered expression of immune system-related genes, as schematically depicted in Supplemental Figure S8.

## Conclusion

This study found that SCGB3A2 deficiency has no significant effects on postnatal lung development/maturation from birth to 8 weeks of age. However, SCGB3A2 may prevent the aging-related destruction of alveoli and therefore the development of emphysematous lung lesions. SCGB3A2 also controls the onset of inflammation of the lungs with the aggregation of lymphocytes accompanied by aging. Thus, SCGB3A2 may be required for the maintenance of homeostasis and immune function in the lungs, which decline with aging. This study also suggested that SCGB3A2 participates in the regulation of *Sftp* expression in older mice.

## Acknowledgments

We would like to thank Kaito Kobori for their technical support (Yamagata Univ. Yamagata, Japan) and Dr. Jerrold Ward for pathological evaluation (Global VetPathology, Maryland, USA). This study was supported by JSPS KAKENHI

(Grant Numbers JP 15K09208, JP 18K08138 to RK), the Smoking Research Foundation Grant Number 2017G023 (to RK), and the National Cancer Institute Intramural Research Program, ZIA BC 010449 (to SK).

## Disclosure

The authors declare that they have no conflict of interests.

## References


1. Niimi T, Keck-Waggoner CL, Popescu NC, et al. UGRP1, a uteroglobin/Clara cell secretory protein-related protein, is a novel lung-enriched downstream target gene for the T/EBP/NKX2.1 homeodomain transcription factor. *Mol Endocrinol*. 2001;15(11):2021–2036. doi:10.1210/mend.15.11.0728
2. Kimura S, Hara Y, Pineau T, et al. The T/ebp null mouse: thyroid-specific enhancer-binding protein is essential for the organogenesis of the thyroid, lung, ventral forebrain, and pituitary. *Genes Dev*. 1996;10:60–69.
3. Yokoyama S, Cai Y, Murata M, et al. A novel pathway of LPS uptake through syndecan-1 leading to pyroptotic cell death. *Elife*. 2018;1:7.
4. Chiba Y, Kurotani R, Kusakabe T, et al. Uteroglobin-related protein 1 expression suppresses allergic airway inflammation in mice. *Am J Respir Crit Care Med*. 2006;173:958–964.
5. Kurotani R, Okumura S, Matsubara T, et al. Secretoglobin 3A2 suppresses bleomycin-induced pulmonary fibrosis by transforming growth factor beta signaling down-regulation. *J Biol Chem*. 2011;286:19682–19692.
6. Cai Y, Winn ME, Zehmer JK, et al. Preclinical evaluation of human secretoglobin 3A2 in mouse models of lung development and fibrosis. *Am J Physiol Lung Cell Mol Physiol*. 2014;306:L10–22.
7. Cai Y, Yoneda M, Tomita T, et al. Transgenically-expressed secretoglobin 3A2 accelerates resolution of bleomycin-induced pulmonary fibrosis in mice. *BMC Pulm Med*. 2015;15:72.
8. Kurotani R, Tomita T, Yang Q, et al. Role of secretoglobin 3A2 in lung development. *Am J Respir Crit Care Med*. 2008;178:389–398.
9. Yokoyama S, Nakayama S, Xu L, et al. Secretoglobin 3A2 eliminates human cancer cells through pyroptosis. *Cell Death Discov*. 2021;7:12.
10. Miele L. Antiflammins. Bioactive peptides derived from uteroglobin. *Ann N Y Acad Sci*. 2000;923:128–140.
11. Johansson S, Andersson K, Wennergren G, et al. CC16 inhibits the migration of eosinophils towards the formyl peptide fMLF but not towards PGD2. *Inflammation*. 2009;32:65–69.
12. Knabe L, Petit A, Vernisse C, et al. CCSP counterbalances airway epithelial-driven neutrophilic chemotaxis. *Eur Respir J*. 2019;1:54.
13. Xu M, Yang W, Wang X, et al. Lung Secretoglobin Scgb1a1 Influences Alveolar Macrophage-Mediated Inflammation and Immunity. *Front Immunol*. 2020;11:584310.
14. Elliott JE, Mantilla CB, Pabelick CM, et al. Aging-related changes in respiratory system mechanics and morphometry in mice. *Am J Physiol Lung Cell Mol Physiol*. 2016;311:L167–176.
15. Fukuda K. Aging of the Respiratory Systems. *Dokkyo j med sci*. 2008;35:219–226.
16. Lang MR, Fiaux GW, Gillooly M, et al. Collagen content of alveolar wall tissue in emphysematous and non-emphysematous lungs. *Thorax*. 1994;49:319–326.
17. Branchfield K, Li R, Lungova V, et al. A three-dimensional study of alveologenesis in mouse lung. *Dev Biol*. 2016;409:429–441.
18. Starcher BC. Elastin and the lung. *Thorax*. 1986;41:577–585.
19. Kuge K, Fujii N, Miura Y, et al. Kinetic study of racemization of aspartyl residues in synthetic elastin peptides. *Amino Acids*. 2004;27:193–197.
20. Le Page A, Khalil A, Vermette P, et al. The role of elastin-derived peptides in human physiology and diseases. *Matrix Biol*. 2019;84:81–96.
21. Kido T, Yoneda M, Cai Y, et al. Secretoglobin superfamily protein SCGB3A2 deficiency potentiates ovalbumin-induced allergic pulmonary inflammation. *Mediators Inflamm*. 2014;2014:216465.
22. Dunnill MS. Quantitative methods in the study of pulmonary pathology. *Thorax*. 1962;17:320–328.
23. Robbesom AA, Versteeg EM, Veerkamp JH, et al. Morphological quantification of emphysema in small human lung specimens: comparison of methods and relation with clinical data. *Mod Pathol*. 2003;16:1–7.
24. Saetta M, Shiner RJ, Angus GE, et al. Destructive index: a measurement of lung parenchymal destruction in smokers. *Am Rev Respir Dis*. 1985;131:764–769.
25. Milner JD, Ward JM, Keane-Myers A, et al. Lymphopenic mice reconstituted with limited repertoire T cells develop severe, multiorgan, Th2-associated inflammatory disease. *Proc Natl Acad Sci U S A*. 2007;104:576–581.
26. Melton DW, McManus LM, Gelfond JA, et al. Temporal phenotypic features distinguish polarized macrophages in vitro. *Autoimmunity*. 2015;48:161–176.
27. Anders S, Pyl PT, Huber W. HTSeq–a Python framework to work with high-throughput sequencing data. *Bioinformatics*. 2015;31:166–169.
28. Love MI, Huber W, Anders S. Moderated estimation of fold change and dispersion for RNA-seq data with DESeq2. *Genome Biol*. 2014;15:550.
29. Ten Have-Opbroek AA. The development of the lung in mammals: an analysis of concepts and findings. *Am J Anat*. 1981;162:201–219.
30. Ward JM. Lymphomas and leukemias in mice. *Exp Toxicol Pathol*. 2006;57:377–381.
31. Beatty K, Bieth J, Travis J. Kinetics of association of serine proteinases with native and oxidized alpha-1-proteinase inhibitor and alpha-1-antichymotrypsin. *J Biol Chem*. 1980;255:3931–3934.
32. Janoff A. Elastases and emphysema. Current assessment of the protease-antiprotease hypothesis. *Am Rev Respir Dis*. 1985;132:417–433.
33. Amy RW, Bowes D, Burri PH, et al. Postnatal growth of the mouse lung. *J Anat*. 1977;124:131–151.
34. Naizhen X, Kido T, Yokoyama S, et al. Spatiotemporal Expression of Three Secretoglobin Proteins, SCGB1A1, SCGB3A1, and SCGB3A2, in Mouse Airway Epithelia. *J Histochem Cytochem*. 2019;67:453–463.
35. Schulte H, Muhlfeld C, Brandenberger C. Age-Related Structural and Functional Changes in the Mouse Lung. *Front Physiol*. 2019;10:1466.
36. Loukov D, Naidoo A, Puchta A, et al. Tumor necrosis factor drives increased splenic monopoiesis in old mice. *J Leukoc Biol*. 2016;100:121–129.
37. de la Higuera L, Lopez-Garcia M, Castro M, et al. Fate of a Naive T Cell: a Stochastic Journey. *Front Immunol*. 2019;10:194.

38. Collins RA, Ikegami M, Korfhagen TR, et al. In vivo measurements of changes in respiratory mechanics with age in mice deficient in surfactant protein D. *Pediatr Res*. 2003;53:463–467.
39. Tokieda K, Whitsett JA, Clark JC, et al. Pulmonary dysfunction in neonatal SP-B-deficient mice. *Am J Physiol*. 1997;273:L875–882.
40. Wert SE, Whitsett JA, Nogee LM. Genetic disorders of surfactant dysfunction. *Pediatr Dev Pathol*. 2009;12:253–274.
41. Korutla L, Strayer DS. SP-A as a cytokine: surfactant protein-A-regulated transcription of surfactant proteins and other genes. *J Cell Physiol*. 1999;178:379–386.
42. Sarker M, Jackman D, Booth V. Lung surfactant protein A (SP-A) interactions with model lung surfactant lipids and an SP-B fragment. *Biochemistry*. 2011;50:4867–4876.
43. Botas C, Poulain F, Akiyama J, et al. Altered surfactant homeostasis and alveolar type II cell morphology in mice lacking surfactant protein D. *Proc Natl Acad Sci U S A*. 1998;95:11869–11874.
44. Glasser SW, Burhans MS, Korfhagen TR, et al. Altered stability of pulmonary surfactant in SP-C-deficient mice. *Proc Natl Acad Sci U S A*. 2001;98:6366–6371.
45. Jin H, Ciechanowicz AK, Kaplan AR, et al. Surfactant protein C dampens inflammation by decreasing JAK/STAT activation during lung repair. *Am J Physiol Lung Cell Mol Physiol*. 2018;314:L882–L892.
46. Mulugeta S, Beers MF. Surfactant protein C: its unique properties and emerging immunomodulatory role in the lung. *Microbes Infect*. 2006;8:2317–2323.